Surface electronic band structure and temperature dependence of the surface state at $\bar{A}$ on Mg(10$\bar{1}$0) surface

S.-J. Tang,[1,2,*] H.-T. Jeng,[3,1,†] Ismail,[4] P. T. Sprunger,[5] and E. W. Plummer[5]

[1]*Department of Physics and Astronomy, National Tsing Hua University, Hsinchu 30013, Taiwan*
[2]*National Synchrotron Radiation Research Center, Hsinchu 30076, Taiwan*
[3]*Institute of Physics, Academia Sinica, Nankang, Taipei 11529, Taiwan*
[4]*Department of Physics and Astronomy, University of Tennessee, Knoxville, Tennessee 37996-1200, USA*
[5]*Department of Physics and Astronomy, Louisiana State University, Baton Rouge, Louisiana 70803, USA*

The surface electronic structure of the Mg(10$\bar{1}$0) surface has been investigated by angle-resolved photoemission around the high-symmetry point $\bar{A}$, where two *sp* Shockley surface states, S1 and S2, have been measured to have the binding energies at $\bar{A}$ of 0.58 and 1.10 eV. The effective mass, m^*/m, of the two surface-state dispersions were determined to be 0.85 and 1.01. First-principles calculations for the S1 and S2 surface states have been performed and show results consistent with experiment. The temperature dependence, the binding energy, and the linewidth of these two surface states were found to be strongly correlated with the bulk. Their behaviors have also been compared with the two surface states at $\bar{A}$ in Be(10$\bar{1}$0).

I. INTRODUCTION

The comparison of experimentally determined and theoretically calculated properties of nearly free-electron metals (NFE) has long been the center of interest due to their simple *sp* electronic structures. In particular, bulk properties of beryllium and magnesium, neighbors at the top of the alkaline-earth metal group, have been investigated experimentally and theoretically.[1] Both have hexagonal-close-packed structures, but compared with beryllium, magnesium's electronic structure is more free electroniclike.[2] Specifically, the lattice c/a ratio of Mg is almost ideal with a value ~1.61 and substantially larger than beryllium, which is anomalously small (~1.56). This reflects a more isotropic electron system in magnesium than beryllium, which has more direction-dependent covalent bonding.[2]

These contrasting bulk physical properties extend to the Mg and Be surfaces. For the hexagonal basal surface, the surface electronic structures, or surface states, of Be(0001), dispersing in a large energy-band gap, are very localized, and dominate the density of states at the Fermi level compared with other NFE metals.[3–5] Moreover, there is a strong electron-phonon coupling of the surface state in Be(0001) which, as determined by angle-resolved photoemission measurements,[6–8] has been found to be three times larger than the bulk value ($\lambda_{surface}$ ~ 0.7). The surface states of Mg(0001) on the other hand, have much longer penetration length into the bulk because they lie much closer to the bulk-band edge.[9,10] Kim *et al.*[11] measured the electron-phonon coupling strength of the surface state in Mg(0001) by analyzing the temperature-dependent linewidth of photoemission spectra and obtained the value 0.27, which is in good agreement with the bulk value. This result was confirmed by Leonardo *et al.*,[12] who implemented *ab initio* calculations. Recently, Chien *et al.*[13] have found anisotropic electron-phonon coupling strength for the surface state in Be(0001).

The explanation of this result is beyond current-theory prediction, which works for Mg(0001). In terms of lattice behavior, Be(0001) has much larger outward first-layer relaxation and thermal expansion than Mg(0001).[14–17]

Differences between the Mg and Be extended beyond the (0001) surfaces. Be(10$\bar{1}$0) possesses very localized surface-electronic structures which are considered to be more covalentlike.[18] Moreover, the surface layer of Be(10$\bar{1}$0) has much larger inward relaxation and thermal contraction than that of Mg(10$\bar{1}$0).[19–22] Hofmann *et al.*[22] proposed a model of directional backbonding to explain the measured large inward relaxation of ~25% between the first layer and the second layer in Be(10$\bar{1}$0). However, Friedel oscillations in the charge density, caused by the redistribution of the electrons to screen the presence of the surface, was considered to be the driving force of oscillatory interplanar relaxation at the Mg(10$\bar{1}$0) surface.[19] Lazzeri *et al.*[23] has used density-functional perturbation theory within quasiharmonic approximation to compare the surface-thermal contraction behaviors of first-second layer spacing between Be(10$\bar{1}$0) and Mg(10$\bar{1}$0). They argued that the change in surface static forces, caused by the bulk-thermal expansion, favors first-layer contraction of Mg(10$\bar{1}$0), while the large anharmonicity of the second-surface layer in Be(10$\bar{1}$0) plays an important role in enhancing the thermal contraction. In an earlier paper,[18] we correlated the surface-electronic structures to the large-surface inward relaxation and thermal-contraction behaviors of Be(10$\bar{1}$0). It is of both interest and importance to examine the electronic structures and their temperature dependence in Mg(10$\bar{1}$0) to understand the interplay between the electronic and lattice behaviors on this surface, which, in contrast to Be(10$\bar{1}$0), should reveal a strong similarity to the bulk. The purpose of this paper is to present experimental results on the electronic structures of Mg(10$\bar{1}$0) determined

by angle-resolved photoemission and compare these results with first-principle calculations to elucidate the underlying behavior of this NFE surface.

II. EXPERIMENTAL AND THEORETICAL DETAILS

The photoemission experiments were performed at the Center for Advanced Microscopic Structures and Device (CAMD) on 6m-TGM Beamline using a high-resolution 150-mm hemispherical Vacuum Scientific Workshop analyzer (VSW HA150).[24] The total resolution from beam and energy analyzer is ~150 meV. In addition, parts of data presented in this paper were taken with He I UV light of photon energy 21.2 eV. The clean Mg($10\bar{1}0$) surface was prepared by cycles of hot sputtering at $T=125\sim150$ °C followed by annealing at $175\sim200$ °C. The cleanliness of Mg($10\bar{1}0$) was confirmed by the sharp low-energy electron diffraction (LEED) pattern of (1×1) unreconstructed-surface and sharp-surface states in the photoemission spectrum.

The band structure calculations were performed using the full-potential projected augmented wave method[25] as implemented in the VASP package[26] within the local-density approximation. The Mg($10\bar{1}0$) surface was simulated using a 240 monolayer (ML) Mg slab (thickness of ~324 Å) with a vacuum thickness of ~10 Å, well separating the slabs. The self-consistent calculations were performed over a 48 k point mesh over the irreducible two-dimensional (2D) Brillouin zone. In our calculation, we found the surface states of Mg($10\bar{1}0$) have long decay length and therefore thick slab of 240 ML is needed to reduce the interaction between the even and odd surface state from two slab surfaces and hence to facilitate the convergence of surface relaxation.[27] The first layer consists of closed packed rows and the crystal may be thought of as a stack of such layers, very similar to an fcc (110) surface. The truncated bulk can be terminated in two ways, either with a short Δd_{12} (short termination) or with a long Δd_{12} (long termination). By optimizing both the short- and long-layer terminations truncated from bulk lattice, the short-layer terminated surface is found to be the true ground state. This is consistent with the previous LEED-IV analysis, which shows a clear preference for the short termination by a lower R factor.[21,22] Our calculations obtained interlayer spacings of $\Delta d_{12,\text{theory}}=-17.50\%$, $\Delta d_{23,\text{theory}}=6.82\%$, $\Delta d_{34,\text{theory}}=-10.18\%$, and $\Delta d_{45,\text{theory}}=3.43\%$, where $\Delta d_{ij}(T)=[d_{ij}(T)-d_{ij}^{\text{bulk}}(T)]/d_{ij}^{\text{bulk}}(T)$ and $d_{ij}^{\text{bulk}}(T)$ refers to the short-layer termination of bulk truncated surface. These results agree very well with previous experimental results of $\Delta d_{12,\text{exp}}=\sim-16\%$, $\Delta d_{23,\text{exp}}=\sim8\%$, $\Delta d_{34,\text{exp}}=\sim-11\%$, and $\Delta d_{45,\text{exp}}=\sim4\%$ from the low-temperature LEED-IV data[21] and the previous computation results,[19,21] thus giving strong confidence in our theoretical approach. Based on the optimized short-layer surface structure, the temperature-dependent band dispersions were then calculated by taking into account the temperature-induced change in interlayer spacing observed in a previous study.[21]
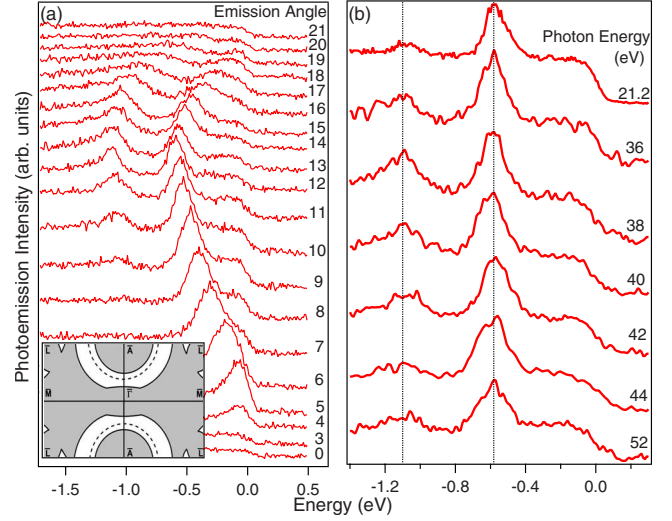

FIG. 1. (Color online) Photoemission spectra (EDCs) taken from Mg($10\bar{1}0$) surface as a function of (1) emission angles at the photon energy 38 eV at $T=90$ K and (2) photon-energy dependence at $\bar{A}$. The inset at the bottom shows the surface Brillouin zone of Mg($10\bar{1}0$), where the shaded area indicates the projection of the bulk-Fermi surface, and the solid curves around $\bar{A}$ are the Fermi contours contributed from S1 surface state.

III. RESULTS AND DISCUSSION

Mg($10\bar{1}0$), as shown in the inset in the Fig. 1, has a rectangular surface Brillouin zone with two major symmetry directions along $\bar{\Gamma}\bar{A}$ (short axis) with 0.603 Å^{-1} in length and $\bar{\Gamma}\bar{M}$ (long axis) with 0.979 Å^{-1} in length, respectively. In this paper, only the electronic-band dispersions along $\bar{\Gamma}\bar{A}$ direction were investigated. Figure 1(a) shows the energy-distribution curves (EDCs) as a function of emission angle along the $\bar{\Gamma}\bar{A}$ direction acquired with an incident photon energy 38 eV. The bottom spectrum (0° emission angle) corresponds to normal emission ($\bar{\Gamma}$ point) and the increasing angles correspond to increasing parallel momentum across the first and second surface Brillouin zones. Two distinct-peak futures are observed to disperse about emission angle ~11.75°, which nominally, at this photon energy, corresponds to the surface-zone boundary $\bar{A}$. The electronic states represented by these two peaks have 2D character due to their symmetry dispersion about the surface-symmetry point. This assessment is confirmed by the photon-energy dependence of these two peaks, as shown in Fig. 1(b), where the two peaks near $\bar{A}$, at 0.58 and 1.10 eV, do not shift in energies with the photon energies from 21.2 to 52 eV. We therefore denote the former as S1 surface state and the later as S2 surface state. The band dispersions of S1 and S2 surface states extracted from Fig. 1 are depicted by symbols (using both data from 38 and 21.2 eV photons) in Fig. 2(a). As opposed to Be($10\bar{1}0$), both surface bands in Mg($10\bar{1}0$) possess parabolic shapes, which reflects free-electronlike properties. The dashed curves represent a fitting of the experimental data assuming a simple free-electron model. The
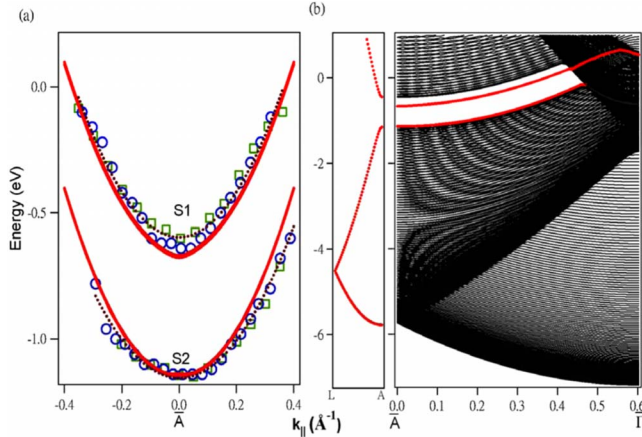
FIG. 2. (Color online) (a) The surface-state band dispersions of S1 and S2 surface states. The square and circle symbols represent the photoemission data taken from photon energy 38 and 21.2 eV, respectively. The dashed curves are the fitting results with a free-electron model. The solid curves are the results of first-principles calculations. (b) The electronic-band structures of Mg(10$\bar{1}$0) surface from the first-principles calculations based on the 240 ML slab model. The two red solid curves, representing S1 and S2 surface-state bands, are the same as those in Fig. 2(a). The inset at the left indicated the calculated bulk-band dispersion from A to L, projected to $\bar{A}$ at the surface Brillouin zone.

experimentally extracted effective mass m^*/m_e is 0.85 for S1 band and 1.01 for S2 band and the Fermi wave vector of S1 band is $k_F=0.366$ Å^{-1}. The solid curves are those from the first-principles calculations based on a 240 ML slab model described above, which match the data reasonably well. The Fermi contour, generated by this calculation, of the S1 surface state is depicted by the dashed curves in the inset of Fig. 1. The measured (calculated) binding energies of S1 and S2 surface states at $\bar{A}$ are 0.58 (0.67) and 1.10 eV (1.14 eV), respectively. The ~0.1 eV discrepancy between the measurement and calculation for the S1 surface state is possibly due to surface quality of the sample and also the theoretical limitations.[18] Figure 2(b) shows the projected calculated bands of Mg(10$\bar{1}$0) along $\bar{\Gamma}\bar{A}$ direction. The inset at the left indicates the calculated bulk-band dispersion from A to L, projected to $\bar{A}$ at the surface Brillouin zone. As seen from the inset, there is a nearly constant projected energy gap at $\bar{A}$, about 0.7 eV in width, which extends across most of the surface Brillouin zone toward $\bar{\Gamma}$. This narrow gap appears to accommodate the S1 and S2 surface-state bands, which, especially S2, nearly coincide with the top and bottom bulk-band edges. At approximately $k_\parallel=0.46$ Å^{-1} from $\bar{A}$, the S1 surface state changes to a resonance in the bulk continuum, dispersing toward the surface-zone center; however the S2 surface state loses its surface character, merging into the bulk-band continuum. Our calculations reveal that the S1 surface state has strong s and p_z symmetry, and S2 has p_y symmetry. Figures 3(a) and 3(b) show the calculated z profiles of charge-density distribution of the S1 and S2 surface states at $\bar{A}$. From the exponential fitting, the extracted decay length from the surface to the bulk is 10 and 25 ML for the
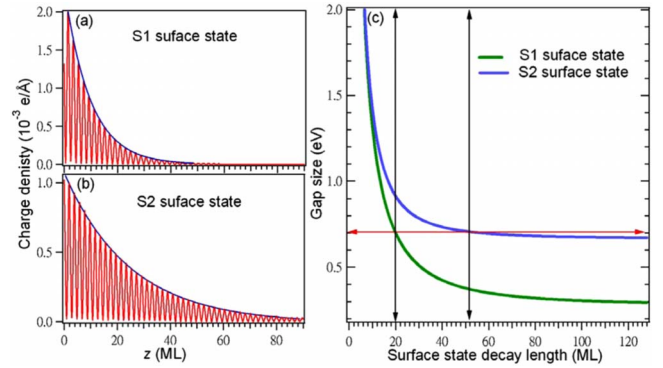

FIG. 3. (Color online) The charge-density z profile for (a) S1 and (b) S2 surface states at $\bar{A}$. The blue solid curves are the exponential fitting of the maximum points. (c) The relationship between the energy-gap size and the surface-state decay length based on one-dimensional nearly free-electron model at the zone boundary.

S1 and S2 charge densities. The decay length of the charge density is one half of that for the amplitude of wave function, which would be 20 and 50 ML, respectively. According to a one-dimensional nearly free-electron model, the decay length of the surface-state wave function can be related to the energy position of surface state and the gap size through the relationship as follows:[28]

$$\mu^2 = -E - \pi^2/a^2 + (V_1^2 + 4\pi^2 E/a^2)^{1/2}, \qquad (1)$$

where $\mu(\geq 0)$ is the imaginary part of the complex wave vector for the surface state, a is the bulk lattice constant along (10$\bar{1}$0) direction, V_1 is the crystal potential of the first order, and E is the energy of the surface state. The relationship between the gap size ($2|V_1|$) and the decay length ($1/\mu$) for both S1 and S2 surface states is depicted in Fig. 3(c), where we have used 2.76 Å for the bulk-lattice constant along (10$\bar{1}$0) direction and calculated energies of S1 and S2 at $\bar{A}$ with respect to the calculated bulk-band bottom (−5.70 eV) along the direction projected to $\bar{A}$. As indicted by the horizontal line in Fig. 3(c), the gap size of 0.7 eV corresponds to the decay length of the surface-state wave function of ~20 ML for S1 and ~52 ML for S2, matching almost identically with results from our first-principles calculation.

Figure 4(a) shows the temperature dependence of the EDCs for the S1 and S2 surface states at $\bar{A}$. The blue solid curves are the fitting results composed of the Gaussian convolution with two Lorentzians for S1 and S2 surface state, another two Lorentzians for the bulk band edges at the top (−0.45 eV) and bottom (−1.15 eV) of the gap, and a polynomial background, convoluted with a Fermi function. The Gaussian function represents the experimental resolution ~150 meV. From such fits, it is possible to extract the energy positions and linewidth for S1 and S2 as a function of temperature, as shown in Figs. 4(b) and 4(c). From a linear fitting, the measured initial energies (empty symbols) of the S1 and S2 states shift in opposite directions with the temperature at the rate of $(-0.364\pm0.12)\times10^{-4}$ and
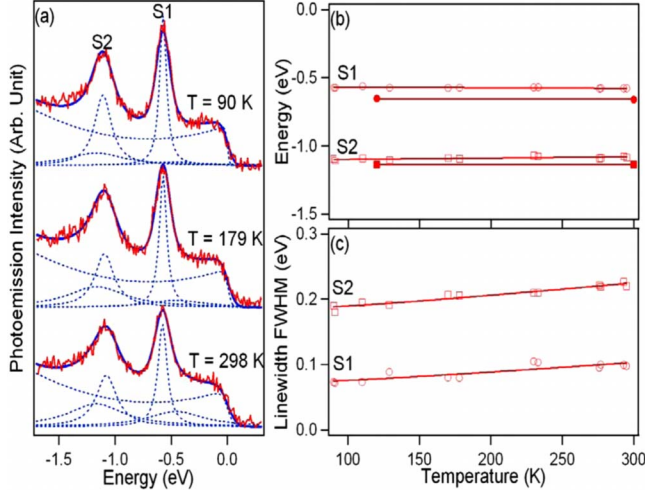
FIG. 4. (Color online) (a) EDCs at $\bar{A}$ at three different temperatures. The red curves are the experimental data; the blue solid curves are the fitting results; and dashed curves give the fit Lorentzians and a background multiplied on a Fermi function. (b) The temperature-dependent energy shifts for S1 (circles) and S2 (squares) surface states: measurement (empty marks) and calculations (filled marks). The sold lines are for linear fits. (c) The temperature-dependent linewidth of S1 (circles) and S2 (squares) surface states. The sold curves are the fitting based on the Debye model with bulk Debye energy 30 meV.

$(0.969 \pm 0.14) \times 10^{-4}$ eV/K, respectively. The filled symbols represent the corresponding initial energies from first-principle calculations according to the LEED-IV measured interlayer spacings of the top layers at temperatures of 120, 300, and 400 K, and the resulting rates of energy shift are $(-0.0328 \pm 0.31) \times 10^{-4}$ and $(0.130 \pm 0.08) \times 10^{-4}$ eV/K for S1 and S2. Although the exact quantities do not compare particularly well, both the measured and calculated results show a consistent trend that with increasing temperature, namely, the S2 surface state shifts toward Fermi level but the S1 surface state shifts away from Fermi level.

Within a quasiparticle picture, the Lorentzian peak in a photoemission spectra can be regarded as a spectral function whose linewidth (W) represents the imaginary part of self-energy, which, in turn, is proportional to the hole inverse lifetime ($1/\tau$) of a surface state. The surface-state hole lifetime is mainly attributed to effects of the electron-electron interaction, electron-phonon interaction, and surface defects. Among the three, the contribution from electron-phonon interaction has the most evident temperature dependence, which is given by the expression[29]

$$W_{e-p}(\omega) = \frac{\hbar}{\tau_{e-p}} = 2\pi\hbar \int_0^{\omega_{max}} \alpha^2 F(\omega')[1 - f(\omega - \omega') + 2n(\omega')$$
$$+ f(\omega + \omega')]d\omega', \qquad (2)$$

where $\alpha^2 F(\omega')$ is the Eliashberg coupling constant, ω_{max} is the maximum phonon frequency, and n and f are the Bose-Einstein and Fermi distribution functions, respectively. Within a Debye model, electron-phonon coupling constant, λ, is linearly related to the Eliashberg coupling constant, $\alpha^2 F(\omega) = \lambda(\frac{\omega}{\omega_D})^2$ if $\omega < \omega_D$, where ω_D is the Debye frequency. Based on this, the linewidths data of S1 and S2 surface states as a function of temperatures, as shown in Fig. 4(c), are then fitted with Eq. (2) by using the Debye model with Mg bulk Debye energy, 30 meV. Employing these constraints yields a reasonable fitting and the resulting electron-phonon coupling constant is nearly equivalent to the bulk value. This result is expected and consistent for surface states with long penetration lengths.[30] As seen, fitting [solid curves in Fig. 4(c)] results in a relatively good agreement to the temperature-dependent linewidth data. Correspondingly, the extracted electron-phonon coupling constant λ is 0.304 ± 0.06 for S1 and 0.391 ± 0.04 for S2, being close to the average bulk value 0.35 ± 0.05 eV.[29] The offset in the fitting, which represents the contributions from electron-electron interaction and surface defects, is about 53 meV for S1 surface state and 160 meV for S2 surface state. The larger offset value for S2 surface state than S1 indicates more scattering channels, especially surface-bulk interband scattering, for S2 surface-state hole in the electron-electron interactions.[31]

A systematic comparison of the S1 and S2 surface states in Mg(10$\bar{1}$0) with those in Be(10$\bar{1}$0), is summarized in Table I.[17–22] According to the previous LEED-IV measurement, the interlayer spacing between the first and second layer for

TABLE I. Comparison between Mg(10$\bar{1}$0) and Be(10$\bar{1}$0) on surface inward relaxation, surface thermal contraction, and the two surface states S1 and S2.

	First layer relaxation	First layer thermal contraction	SS decay length	Energy shift (relaxation)	Energy shift (thermal contraction)	EP coupling constant λ
Mg(10$\bar{1}$0)	-14.5% [a]	$\Delta d_{12}/\Delta T = -0.015\%$ (1/K)[c]	S1 20 ML[e] S2 52 ML[e]	S1 5.5 meV[e] S2 6.0 meV[e]	S1 ($\Delta E/\Delta T$) -0.364×10^{-4} eV/K [e] S2 ($\Delta E/\Delta T$) 0.969×10^{-4} eV/K [e]	S1 0.304[e] S2 0.391[e]
Be(10$\bar{1}$0)	-25% [b]	$\Delta d_{12}/\Delta T = -0.019\%$ (1/K)[d]	S1 4 ML[f] S2 6 ML[f]	S1 29 meV[f] S2 178 meV[f]	S1 ($\Delta E/\Delta T$) -0.61×10^{-4} eV/K [f] S2 ($\Delta E/\Delta T$) 1.71×10^{-4} eV/K [f]	S1 0.646[f] S2 0.491[f]

[a]Reference 19.
[b]Reference 22.
[c]Reference 21.
[d]Reference 17.
[e]Present work.
[f]Reference 18.

Mg($10\bar{1}0$) surface has -14.5% inward relaxation, which was consistent with the first-principles calculation.[19] Friedel oscillations, creating a charge modulation of wavevector $2k_F$ from the surface into the bulk, were considered to be the driving force for the oscillatory interplanar relaxation in Mg($10\bar{1}0$).[19] The calculation in this work indicates both S1 and S2 surface states show almost no shift in energies upon relaxation in stark contrast to Be($10\bar{1}0$) wherein S1 and, specially, S2 surface states shift in energy.[18] Therefore, as opposed to Be($10\bar{1}0$), the S1 and S2 surface states in Mg($10\bar{1}0$) are not to be considered the driving mechanism of the large surface relaxation. This is to be expected due to the long decay lengths, 20 and 52 ML, of S1 and S2 surface states, which are not as sensitive to the lattice changes in the top surface layers. Regarding the surface-thermal contractions, the contraction rate with the temperature for the Mg($10\bar{1}0$) is $d_{12}/\Delta T = -0.015\%$ (1/K), which is slower than the rate -0.019% (1/K) for Be($10\bar{1}0$).[17] According to the photoemission results in this paper, the S1 surface state in Mg($10\bar{1}0$) shifts toward higher binding energy with increasing temperature, which is the same direction as S1 in Be($10\bar{1}0$), but with slower rate. Slower rates of both surface-thermal contraction and S1 surface-state energy shift in Mg($10\bar{1}0$) than those in Be($10\bar{1}0$) imply relatively smaller contribution to the surface-lattice behavior by the surface states in Mg($10\bar{1}0$). This assessment is in agreement with the conclusion made by Lazzeri *et al.*[23] that the thermal contraction of the interlayer spacing between the first and the second layer in Mg($10\bar{1}0$) is mainly due to a mechanism originating from the static contribution that thermal bulk-lattice expansion in the in-plane direction leads to a change in the static interlayer forces. The electron-phonon coupling constants λ extracted from S2 is larger than that of S1 in Mg($10\bar{1}0$). This result is opposite to that of Be($10\bar{1}0$), where more localized S1 surface state has larger λ value than S2.[18] The discrepancy of the surface-state electron-phonon coupling between Mg($10\bar{1}0$) and Be($10\bar{1}0$) can be understood in terms of the different surface-and-bulk relationships of these two surfaces. As for Be($10\bar{1}0$), the surface is almost decoupled from the bulk with respect to both electronic or lattice structures. Therefore, the scenario that localized surface states and localized surface phonons would have larger probability to interact with each other, triggered by the reduced symmetry, is more likely for Be($10\bar{1}0$) than Mg($10\bar{1}0$), as indicated by the much higher value of λ for S1 surface state than the values for S2 surface state and bulk. However, for Mg($10\bar{1}0$), the intimate relationship between the bulk and surface leads to a different scenario in that surface state with longer decay length from the surface to the bulk would couple with more bulk phonons in addition to surface phonons. Matzdorf *et al.*[32] has attributed the higher λ value, 0.137, of sp-like Shockley state at $\bar{\Gamma}$ on Cu(111) than that of d-like Tamm state at $\bar{M}$ ($\lambda = 0.09$) to the different spatial extent of the surface states. The bulk projected band gap in the noble-metal surface as well as Mg($10\bar{1}0$) is very small so that the behavior of the Shockley surface state in the gap is dominated greatly by the bulk state at the bulk-band edge.

IV. CONCLUSIONS

We have studied the surface-electronic structures of Mg($10\bar{1}0$) in the symmetry direction from $\bar{\Gamma}$ to $\bar{A}$ by angle-resolved photoemission. Two surface states, S1 and S2, were identified, and their energy-band dispersions and temperature dependence were investigated and compared to first-principle calculations. According to the comparison of S1 and S2 surface states with their counterparts in Be($10\bar{1}0$), we find the surface properties of Mg($10\bar{1}0$) are strongly linked to the bulk. Therefore, the surface states on Mg($10\bar{1}0$) have less interplay with the surface lattice behaviors than those in Be($10\bar{1}0$).

*sjtang@phys.nthu.edu.tw

†jeng@phys.sinica.edu.tw

[1] E. W. Plummer, Phys. Scr. **T17**, 186 (1987).

[2] M. Y. Chou, P. K. Lam, and M. L. Cohen, Phys. Rev. B **28**, 4179 (1983); M. Y. Chou and M. L. Cohen, Solid State Commun. **57**, 785 (1986).

[3] R. A. Bartynski, E. Jensen, T. Gustafsson, and E. W. Plummer, Phys. Rev. B **32**, 1921 (1985).

[4] I. Vobornik, J. Fujii, M. Mulazzi, G. Panaccione, M. Hochstrasser, and G. Rossi, Phys. Rev. B **72**, 165424 (2005).

[5] I. Vobornik, J. Fujii, M. Hochstrasser, D. Krizmancic, C. E. Viol, G. Panaccione, S. Fabris, S. Baroni, and G. Rossi, Phys. Rev. Lett. **99**, 166403 (2007).

[6] M. Hengsberger, D. Purdie, P. Segovia, M. Garnier, and Y. Baer Phys. Rev. Lett. **83**, 592 (1999); M. Hengsberger, R. Fresard, D. Purdie, P. Segovia, and Y. Baer, Phys. Rev. B **60**, 10796 (1999).

[7] T. Balasubramanian, E. Jensen, X. L. Wu, and S. L. Hulbert, Phys. Rev. B **57**, R6866 (1998).

[8] S. LaShell, E. Jensen, and T. Balasubramanian, Phys. Rev. B **61**, 2371 (2000).

[9] R. A. Bartynski, R. H. Gaylord, T. Gustafsson, and E. W. Plummer, Phys. Rev. B **33**, 3644 (1986).

[10] F. Schiller, M. Heber, V. D. P. Servedio, and C. Laubschat, Phys. Rev. B **70**, 125106 (2004).

[11] T. K. Kim, T. S. Sorensen, E. Wolfring, H. Li, E. V. Chulkov, and P. Hofmann, Phys. Rev. B **72**, 075422 (2005).

[12] A. Leonardo, I. Yu. Sklyadneva, V. M. Silkin, P. M. Echenique, and E. V. Chulkov, Phys. Rev. B **76**, 035404 (2007).

[13] Teyu Chien, E. Rienks, M. F. Jensen, Ph. Hofmann, and E. W. Plummer (unpublished).

[14] H. L. Davis, J. B. Hannon, K. B. Ray, and E. W. Plummer, Phys. Rev. Lett. **68**, 2632 (1992).

[15] K. Pohl, J.-H. Cho, K. Terakura, M. Scheffler, and E. W. Plummer, Phys. Rev. Lett. **80**, 2853 (1998).

[16] P. T. Sprunger, K. Pohl, H. L. Davis, and E. W. Plummer, Surf. Sci. **297**, L48 (1993).

[17] Ismail, Ph. Hofmann, A. P. Baddorf, and E. W. Plummer, Phys. Rev. B **66**, 245414 (2002).

[18] S.-J. Tang, Ismail, P. T. Sprunger, and E. W. Plummer, Phys. Rev. B **65**, 235428 (2002); S.-J. Tang, H.-T. Jeng, Chen-Shiung Hsue, Ismail, P. T. Sprunger, and E. W. Plummer, *ibid.* **77**, 045405 (2008).

[19] J.-H. Cho, Ismail, Z. Zhang, and E. W. Plummer, Phys. Rev. B **59**, 1677 (1999).

[20] P. Staikov and T. S. Rahman, Phys. Rev. B **60**, 15613 (1999).

[21] Ismail, E. W. Plummer, Michele Lazzeri, and Stefano de Gironcoli, Phys. Rev. B **63**, 233401 (2001).

[22] Ph. Hofmann, K. Pohl, R. Stumpf, and E. W. Plummer, Phys. Rev. B **53**, 13715 (1996).

[23] M. Lazzeri and Stefano de Gironcoli, Phys. Rev. B **65**, 245402 (2002).

[24] K. Koch, Ph.D. thesis, University of Texas Austin, 2001.

[25] P. E. Blochl, Phys. Rev. B **50**, 17953 (1994); G. Kresse and D. Joubert, *ibid.* **59**, 1758 (1999).

[26] G. Kresse and J. Hafner, Phys. Rev. B **48**, 13115 (1993); G. Kresse and J. Furthmuller, Comput. Mater. Sci. **6**, 15 (1996); Phys. Rev. B **54**, 11169 (1996).

[27] V. Chis and B. Hellsing, Phys. Rev. Lett. **93**, 226103 (2004).

[28] G. Sydney, *Davison and Maria Steslicka, Basic Theory of surface states* (Oxford University Press, New York, 1992).

[29] G. Grimvall, *The Electron-Phonon Interaction in Metals* (North-Holland, New York, 1981).

[30] B. A. McDougall, T. Balasubramanian, and E. Jensen, Phys. Rev. B **51**, 13891 (1995).

[31] V. M. Silkin, T. Balasubramanian, E. V. Chulkov, A. Rubio, and P. M. Echenique, Phys. Rev. B **64**, 085334 (2001).

[32] R. Matzdorf, G. Meister, and A. Goldmann, Phys. Rev. B **54**, 14807 (1996).